J Mater Sci: Mater Med (2011) 22:2207–2218
DOI 10.1007/s10856-011-4402-8

Preparation and characterization of electrospun PCL/PLGA membranes and chitosan/gelatin hydrogels for skin bioengineering applications

Rose Ann Franco · Thi Hiep Nguyen · Byong-Taek Lee

Received: 12 January 2011 / Accepted: 18 July 2011 / Published online: 31 July 2011

Abstract In this study, two distinct systems of biomaterials were fabricated and their potential use as a bilayer scaffold (BS) for skin bioengineering applications was assessed. The initial biomaterial was a polycaprolactone/poly(lacto-co-glycolic acid) (PCL/PLGA) membrane fabricated using the electrospinning method. The PCL/PLGA membrane M-12 (12% PCL/10% PLGA, 80:20) displayed strong mechanical properties (stress/strain values of 3.01 ± 0.23 MPa/225.39 ± 7.63%) and good biocompatibility as demonstrated by adhesion of keratinocyte cells on the surface and ability to support cell proliferation. The second biomaterial was a hydrogel composed of 2% chitosan and 15% gelatin (50:50) crosslinked with 5% glutaraldehyde. The CG-3.5 hydrogel (with 3.5% glutaraldehyde (v/v)) displayed a high porosity, ≥97%, good compressive strength (2.23 ± 0.25 MPa), ability to swell more than 500% of its dry weight and was able to support fibroblast cell proliferation. A BS was fabricated by underlaying the membrane and hydrogel casting method to combine these two materials. The physical properties and biocompatibility were preliminarily investigated and the properties of the two biomaterials were shown to be complementary when combined. The upper layer membrane provided mechanical support in the scaffold and reduced the degradation rate of the hydrogel layer. Cell viability was similar to that in the hydrogel layer which suggests that addition of the membrane layer did not affect the biocompatibility.

R. A. Franco · T. H. Nguyen · B.-T. Lee (✉)
Department of Biomedical Engineering and Materials, College of Medicine, Soonchunhyang University, Cheonan 330-090, Korea
e-mail: lbt@sch.ac.kr

1 Introduction

Tissue engineering is a multidisciplinary field which aims to regenerate native tissues from viable sources [1]. It provides an alternative treatment for terminal clinical conditions when tissue or organ transplantation is not available. With the emergence of artificial skin, acute cases such as burns and chronic cases like congenital nevi, disabling scars and skin ulcerations are greatly benefited [2]. Artificial skin scaffolds should be able to function as cover to protect the wound against infection while allowing oxygen to permeate and to stimulate fibroblast activity towards healing [3]. It must protect the wound against fluid loss and provide a moist environment for rapid epithelialization [4]. It must be biocompatible and physiologically degradable as it encourages native skin cells to grow. Ideally, it should be able to withstand mechanical stress during implantation.

Native skin is composed of two layers with distinct qualities. Thus, a BS should more accurately mimic the physical structure of the normal skin. One of the most used, commercially-available dermal substitute is Integra, which is a BS composed of a silicone upper layer and a collagen-glycosaminoglycan porous sublayer. The two separate layers in the bilayer structure have distinct functions which help it adapt to the complex environment of wound healing. The upper, dense layer serves as primary wound cover and the lower biodegradable, porous layer allows for the influx of native cells growth while maintaining moisture on the wound bed. In constructing a bilayer structure, the separate materials should first be characterized in order to determine its suitability as a tissue engineering scaffold.

The initial biomaterial that will comprise the upper dense layer is fabricated through electrospinning method. Electrospinning is a relatively simple technique of producing nano-scale fibers [5] and is highly efficient in

providing high surface area to volume ratios producing an extracellular matrix-like scaffold [6, 7]. A wide range of natural and synthetic polymers can be used to fabricate electrospun skin scaffolds. The combination of poly (lactic-co-glycolic acid) (PLGA) and increasing concentrations of polycaprolactone (PCL) was investigated in this study. PCL is a polyester that exhibits good mechanical properties [8], is atoxic [9] and can minimally support keratinocyte growth and proliferation [10]. PCL, however, is hydrophobic, contains very few cell recognition sites and degrades slowly [11]. In this regard, PLGA was combined to increase the biodegradability and biocompatibility of the material. PLGA is more tolerated by the human body since its two components, lactic acid and glycolic acid, are excreted physiologically [12, 13].

The second biomaterial that will eventually comprise the lower porous layer is a hydrogel consisting of chitosan and gelatin. Chitosan–gelatin blends in hydrogels are commonly used because of their individual characteristics, which are favorable for biological growth and structural strength [14–18]. Chitosan, a natural polymer obtained from the deacetylation of chitin, has a widespread application in tissue engineering due to its anti-microbial properties, high biodegradability, biocompatibility and ability to aid in wound healing and angiogenesis [19]. Gelatin is a widely-used, water-soluble natural polymer derived from thermal denaturation of collagen and it displays low antigenicity and high biocompatibility and bioabsorptivity [20].

In this study, the physical properties, mechanical integrity and biocompatibility of two separate biomaterials were investigated. Morphological characterization was done through SEM, determination of porosity by mercury intrusion porosimetry and density calculations. The mechanical strength of the materials was examined to determine which sample condition can withstand the applied stress. Biodegradation was investigated by immersing the samples in PBS for 25 days to determine mass lost over time. The amount of moisture that can be absorbed by the hydrogel was determined by swelling studies in a span of 160 min. Cytotoxicity tests, cell proliferation studies and visualization of cell adhesion were done to check the biocompatibility of the scaffolds in vitro. The results of the tests performed determined which conditions were optimums and were used to construct the BS that will be eventually used for skin tissue engineering applications.

2 Materials and methods

2.1 Materials

Chitosan (85% deacetylation, from crab), gelatin (from porcine skin), PLGA (85:15), PCL (Mn 80,000), tetrahydrofuran (THF, minimum 99%), dimethylformamide (DMF, 99%) from Sigma-Aldrich, USA. Dimethysulfoxide (DMSO, 99.0%) from Samchun Pure Chemical Co., LTD, Korea. (3-(4,5-Dimethylthiazol-2-yl)-2,5-diphenyltetrazolium bromide (MTT) solution from Sigma. L929 cell line was obtained from ATCC cell line (CCL-1^{TM}, NCTC clone 929 [L cell, L929, derivative of Strain L]). Human keratinocytes from neonatal foreskin were purchased from Dail Scientific Trade, Inc, Korea. The water used in the entire experiment was deionized through Milli-Q System (Millipore, USA). All other chemicals used were of reagent grade.

2.2 Preparation of samples

2.2.1 Electrospun PCL/PLGA membranes

The electrospun membranes were prepared according to a previous study in our laboratory with modifications [21]. PCL was separately dissolved in THF:DMF:MC (40:40:20) solvent to obtain 12, 13 and 14% (wt/vol%). PLGA was dissolved in the same solvent to obtain a 10% solution (Table 1). These mixtures were mechanically stirred until completely dissolved in their respective solvents. Different concentrations of these solutions were later combined to achieve a ratio of 80:20 (PCL/PLGA), 4 ml, and mechanically stirred again for 12 h at ambient temperature until the solution appeared completely homogenous. The membranes were fabricated using an electrospinning machine (NNC 30 kV-2 mA portable type, Nano NC, Korea) at a voltage supply of 25.0 kV. A Luer-lock syringe (12 ml) was used with a 25-gauge needle for electrospinning. The solution flow rate was regulated at 0.50 ml/h and a distance of 20 cm from the collector and ejecting needle. Spraying distance was also regulated at 160 mm on the Y-axis of the electrospinning machine. The electrospun membranes were placed in a bottle of diethylether with a magnetic stirrer overnight to remove the excess solvent.

2.2.2 Chitosan–gelatin hydrogel

Chitosan (85% deacetylation, from crab) was dissolved in a 1% acetic acid solution to achieve a concentration of 2% (wt/vol%). The solution was stirred mechanically for 24 h. Minute particles remained after sufficient stirring, therefore, the solution was filtered prior to use. Gelatin (from porcine skin) was dissolved in deionized water (Milli-Q) to achieve a 15% w/v solution. The two solutions were combined and mechanically stirred prior to addition of crosslinking agent. Glutaraldehyde (GA) stock, 25%, was diluted to achieve a 5% solution. This was poured into the chitosan–gelatin mixture in different volumes to achieve varying percentage content of glutaraldehyde concentrations relative to

Table 1 Composition and physical characterization of electrospun PCL/PLGA membranes

Samples	PCL (%)	PLGA (%)	Fiber diameter (μm)	Thickness (μm)	Density (g/cm^3)	Stress at break (MPa)	Strain at break (%)
M-12	12	10	0.975 ± 0.402	144.65 ± 4.99	10.21 ± 0.96	3.01 ± 0.23	225.39 ± 7.63
M-13	13	10	1.213 ± 0.539	287.78 ± 8.86	11.42 ± 4.43	2.26 ± 0.30	116.03 ± 34.56
M-14	14	10	1.689 ± 0.707	420.23 ± 14.21	12.22 ± 0.57	2.05 ± 0.28	72.84 ± 19.56

Table 2 Composition and physical characterization of chitosan–gelatin hydrogels

Samples	5% GA content (%)	2% Chitosan (%)	15% Gelatin (%)	Density (g/cm^3)	Porosity (%)	Average pore diameter (μm)	Compressive strength (MPa)
CG-3	3	50	50	0.125 ± 0.014	97.5	240 ± 114	1.03 ± 0.12
CG-3.5	3.5	50	50	0.125 ± 0.002	97.485	290 ± 109	2.23 ± 0.25
CG-4	4	50	50	0.112 ± 0.010	97.661	235 ± 135	2.73 ± 0.60
CG-4.5	4.5	50	50	0.112 ± 0.003	97.542	272 ± 138	3.02 ± 1.01
CG-5	5	50	50	0.115 ± 0.002	97.555	264 ± 134	3.50 ± 0.94

chitosan–gelatin mixture (3, 3.5, 4, 4.5 and 5%) (Table 2). All hydrogels were poured into polysterene tissue culture plates (Falco), pre-freezed at −20°C for 12 h then lyophilized in a freeze drying machine (Ilshin Lab, Co. Ltd., Korea) at −81°C, 5 mTorr for 36 h.

2.2.3 Bilayer scaffold

Following the characterization of the electrospun PCL/PLGA membranes and chitosan–gelatin hydrogels, the M-12 membrane and CG-3.5 hydrogel were shown to display favorable physical properties and cell-material interactions. A BS was fabricated using these two materials by underlaying and casting method. M-12 was fabricated and was laid in a 6-well TCP to which 5 ml of CG-3.5 was then poured. The resulting samples were pre-freezed then freeze-dried under the above-mentioned conditions.

2.3 Characterization of samples

2.3.1 Morphology

Squares of 1 cm × 1 cm were cut from the electro-spun PCL/PLGA membranes and lyophilized chitosan–gelatin hydrogel samples were sputtered with a platinum sputter coater (Cressington Sputter Coater). Samples were then viewed using a field emission scanning electron microscope (JSM701F, JEOL, Japan) at an acceleration voltage of 15 kV.

The average fiber diameter ($n = 60$) and membrane thickness was determined by examining the cross-sections taken at different areas for each sample. All measurements were done using SEM-assisted image analysis software.

The average pore diameters of the CG hydrogels were determined from cross-sections of three random samples of each hydrogel taken at different areas. At least 100 pores were analyzed for each CG hydrogel.

The density of the samples was calculated by dividing the obtained mass by the calculated volume (length × width × height). Average values were obtained from four replicates with standard deviation.

2.3.2 Mechanical strength

The mechanical strength of a scaffold determines the stress it can withstand before it undergoes significant contraction. This intensive property of a material is measured as the force causing the breakage on the material divided by the cross-sectional area of the sample. During the time a material undergoes stress, it undergoes deformation where particles are relatively displaced. This deformational change is the material strain and is expressed as a percentage.

A universal testing machine (Unitech^{TM}, R&B, Korea) was used in testing the mechanical strength of the fabricated membranes, hydrogels and BS. An accompanying Helio-X software program determined the stress and strain values of the materials. Rectangular strips of 33 mm × 2 mm × T (where T is the thickness) were cut from each fabricated electrospun PCL/PLGA membrane. The ends of the membrane strips were glued to a paper frame to anchor it to the tensile tester. The sides of the frame were cut upon application of strain at crosshead speed of (1 mm/min) with a 500-g load cell.

Compressive strength was measured to determine the strength of the 3D scaffold when uniaxial strength is applied. Samples of the CG hydrogels were cut to dimensions of 7 mm × 7 mm × 5 mm for all tests done in this study, unless stated otherwise. Wet samples of CG hydrogels were used to determine its compressive strength.

A uniaxial displacement was applied to the specimen at a crosshead speed of 0.5 mm/min and the load was measured with a 20-g load cell. Reported results were the average of five trials with standard deviation.

2.3.3 Swelling ability of chitosan–gelatin hydrogels

CG hydrogel samples and BSs were pre-weighed then immersed in phosphate buffer solution, pH 7.4, 37°C, at different time intervals. Swelling ratio (SR), which was expressed as a percentage, was calculated as follows:

$$\mathrm{SR}(\%) = \frac{(W_x - W_0) \times 100}{W_0}$$

where W_0 was the initial weight prior to experimentation and W_x was the weight measured after each observation time.

2.3.4 Porosity

The porosity of the samples was determined using mercury intrusion porosity meter (Quantachrome Porosity Meter, FL, USA). CG hydrogels, 5 mm × 5 mm × 3 mm, were placed inside quartz penetrometers after sufficient drying and the porosity was determined using the accompanying Poremaster software.

2.3.5 In vitro biodegradation

Lyophilized CG hydrogel samples, at the dimensions described above and electrospun PCL/PLGA membranes (25 mm × 20 mm) and BSs were pre-weighed then immersed in phosphate buffer solution, pH 7.4, 37°C, for a 25-day observation. PBS was replaced every week. After each observation time, the samples were freeze-dried for 6 h and the remaining weight was measured after 5, 10, 15, 20 and 25 days. The degree of degradation was calculated as follows,

$$\text{Degree of degradation } (\%) = \frac{(W_0 - W_t) \times 100}{W_0}$$

where W_0 was the original weight and W_t was the weight per time interval. All samples were tested four times each for every observation time. In the case of PCL/PLGA membranes, mass retention was computed as the ratio of weight during a sampling day against the original weight.

2.3.6 Cytotoxicity

Samples (CG hydrogels, electrospun PCL/PLGA membranes and BS) were incubated in 5 ml RPMI media with 10% (v/v) of fetal bovine serum (FBS) and 1% penicillin/streptomycin antibiotics for 3 days at 37°C, while shaking at 100 rpm in an incubator to obtain an extract solution. Fibroblast cells, 1×10^4 cells/100 µl, were seeded in 96-well culture plates then incubated for 24 h at 37°C, 5% CO_2. Extract solutions were filtered with 0.20 µm filters then diluted to the following concentrations relative to fresh media: 12.5, 25, 50 and 100%. Diluted extract solutions were added to the cell-seeded tissue culture plates and incubated for another 3 days at 37°C and 5% CO_2. Cell-seeded wells without an extract solution (0%) were also prepared as a control. MTT solution was added to the wells after 3 days and re-incubated for 4 h. Media was discarded from the wells and replaced with 200 µl of DMSO to dissolve the formazan salts. Cell viability was quantified by measuring the absorbance at 595 nm using an ELISA reader (Turner Biosystems CE, Promega Corporation, USA). These experiments were conducted in four replicates and cell viability was calculated as percentage relative to the cell-seeded wells containing media without the extract solution.

2.3.7 Cell proliferation

Fibroblast cells, 1×10^4 cells/ml, were seeded on the electrospun PCL/PLGA membranes that were 15 mm in diameter, and CG hydrogel samples that were 8 mm × 8 mm × 1.5 mm and incubated for 1, 3 and 5 days in 24-well culture plates. Media was replaced every other day. After each incubation time, media was discarded and MTT solution was added and re-incubated for another 4 h. DMSO was then added and plates were shaken for 1 h and the absorbance was read at 595 nm using an ELISA plate reader. Cell viability was calculated as the ratio of absorbance to the control after 1 day of incubation and expressed as a percentage.

2.3.8 Cell adhesion behavior

SEM visualization of cell adhesion behavior was done by seeding electrospun PCL/PLGA membranes with keratinocyte cells, 1×10^4 cells/ml, and CG hydrogel with fibroblast cells, 1×10^4 cells/ml, after sufficient sterilization with 70% ethanol. Samples were incubated for 1 and 3 days. Fixation was done using 2% glutaraldehyde for 15 min, increasing alcohol series (50, 60, 70, 80, 90, 95 and 100%) for dehydration and hexamethyldisilazane (HMDS) twice for critical point drying. Dried cell-seeded samples were sputtered and examined by scanning electron microscopy. Polysterene coverslips were used as control for this test.

2.4 Statistical analysis

Characterization tests were done in four replicates, unless otherwise stated. Values were expressed as the mean of

four replicates and standard deviation. Experimental results done in a continuous time interval were also analyzed by one-way ANOVA, single factor with a confidence level of $P \geq 0.05$ using Microsoft Excel 2007 to determine if the changes were statistically significant.

3 Results

3.1 Electrospun PCL/PLGA membranes

3.1.1 Morphology

Fibers appeared distinctly separated and randomly interspersed. Individual fibers were found to be cylindrical and continuous. Further investigation on the morphology of the fibers revealed that the average fiber diameter and fiber diameter frequency distribution varied among the samples. M-12 (Fig. 1a) had an average fiber diameter of 975 ± 402 nm and more than 60% of the fibers examined ($n = 60$) had a diameter below 1,000 nm. M-13 (Fig. 1b) had an average fiber diameter of 1,213 ± 539 nm and M-14 (Fig. 1c) had an average fiber diameter of 1,689 ± 707 nm. Analysis of the frequency of the fiber distribution showed that an increased PCL concentration resulted to a shift in the frequency of the fiber size towards the larger diameter.

The average thickness of the membranes was also measured after the spraying distance of the syringe nozzle in the electrospinning machine was calibrated to 160 mm and the volume of the solution at 4 ml. In these experiments, the thickness of the membrane was shown to vary as a function of PCL concentration where the thickness of the cross-section of the membranes increased as the concentration of the PCL increased. Consequently, there was a corresponding increase in density when the membrane thickness increased (Table 1).

3.1.2 Mechanical strength

The PCL/PLGA membranes are two-dimensional scaffolds that usually undergo breakage from the application of stress by means of pulling or stretching the membrane. The amount of uniaxial stress applied was quantified by measuring the tensile strength. An increased concentration of PCL lowered the tensile strength, and the elongation of the membrane was more evident (Fig. 2a). The tensile strength of M-12, M-13 and M-14 was 3.01 ± 0.23, 2.26 ± 0.30 and 2.05 ± 0.28 MPa, respectively. A low tensile strength breaks the membrane before it can further elongate. Thus, the strain values were also reduced for the membranes with increasing PCL concentration. M-12 showed the highest strain value of 225.39 ± 7.63% (Fig. 2). M-13 and M-14 had strain at break values that are 116.03 ± 34.56 and 72.84 ± 19.56%, respectively. All of these results are numerically presented in Table 1.

3.2 Chitosan–gelatin hydrogel

3.2.1 Morphology

Figure 3 showed the SEM photomicrographs of hydrogels at different GA concentrations. The porosity was determined to be around 97% for all samples. The average pore diameter ranged from 235 ± 135 to 290 ± 109 μm. Density values were 0.112 ± 0.003 to 0.125 ± 0.014 g/cm^3 (Table 2).

3.2.2 Mechanical strength

Three-dimensional scaffolds like the CG hydrogels fabricated in this study may undergo compression stresses during handling. Thus, the compressive strength was tested. Figure 4 showed the values obtained after application of uniaxial displacement to the samples and was measured with a 20-g load cell. The minimum compressive strength was 1.03 ± 0.12 MPa for CG-3 and the maximum was 3.50 ± 0.94 MPa for CG-5. An increasing compressive strength was observed as the amount of crosslinker was increased.

3.2.3 Swelling ability

The swelling behavior of CG hydrogels was shown in Fig. 5. All CG hydrogels swelled to more than 100% of their dry weight within 15 min and continued to swell for up to 75–90 min of observation when the swelling rate relatively slowed down. Notably, CG-3, which contained the lowest GA content, swelled fastest at more than 300% of its original weight in the first 15 min. It continued to swell to more than 600% of its weight until the end of 160 min of observation. The other hydrogels plotted swelling values between CG-3 and CG-5.

3.2.4 In vitro biodegradation

The biodegradation of the PCL/PLGA membranes and CG hydrogels were observed for 25 days. No statistically significant weight change in the membranes ($P \geq 0.05$) was found throughout the time of observation (Fig. 6a). In the case of CG hydrogels, it was observed that the amount of crosslinker affected the degradation time of the scaffolds. During the time of observation, there was a significant weight change for every CG hydrogel sample indicating

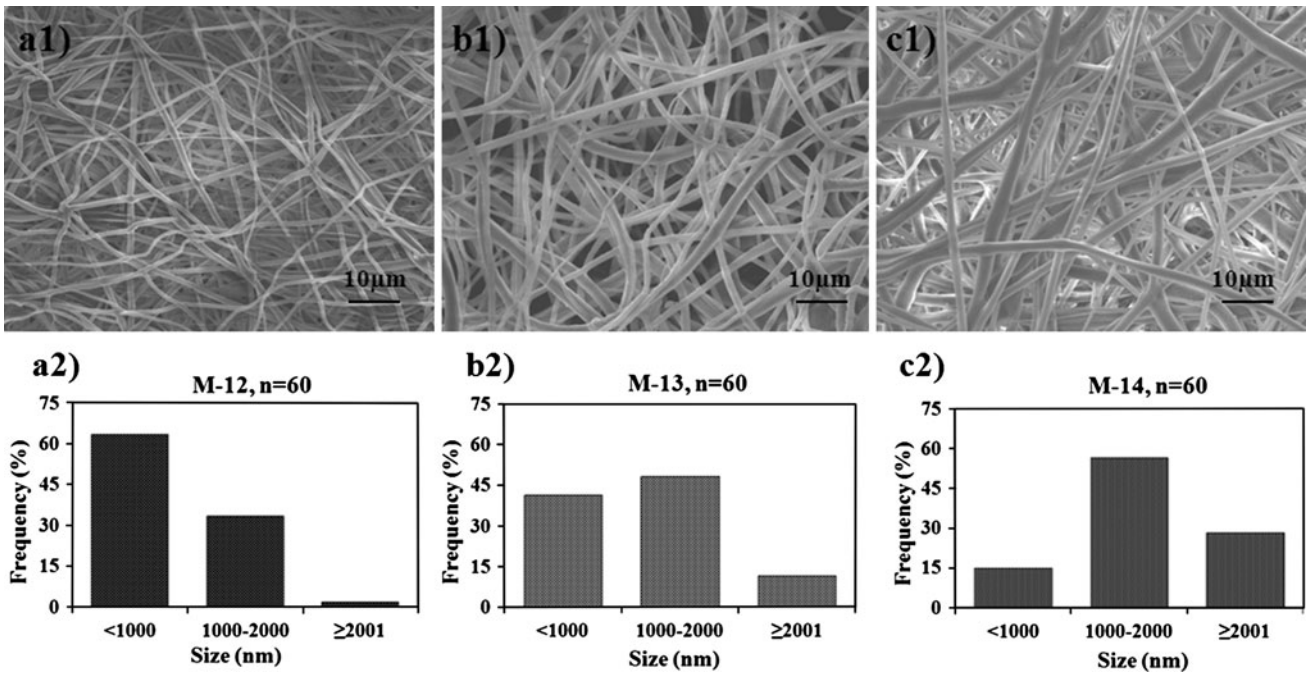

Fig. 1 SEM micrographs (**1**) and fiber diameter distribution (**2**) of PCL/PLGA membranes with increasing PCL concentration. **a** M-12 (12% PCL), **b** M-13 (13% PCL) and **c** M-14 (14% PCL)

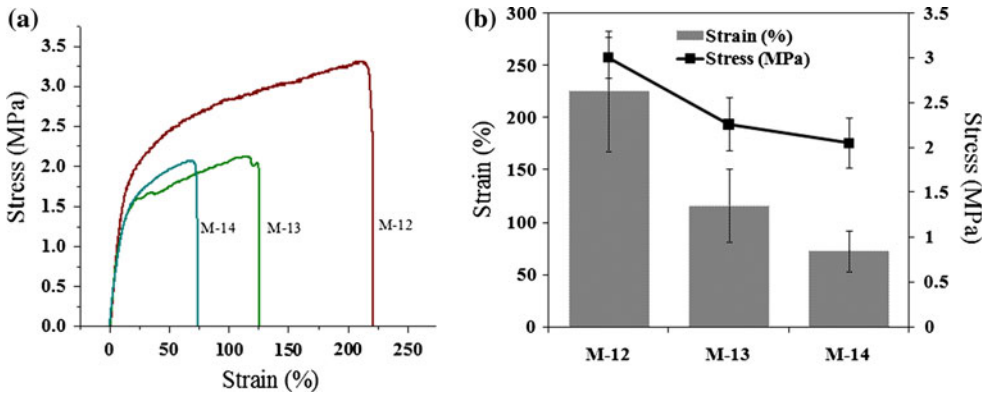

Fig. 2 Stress–strain curves of PCL/PLGA membranes (**a**). Stress and strain at break (**b**) of electrospun membranes

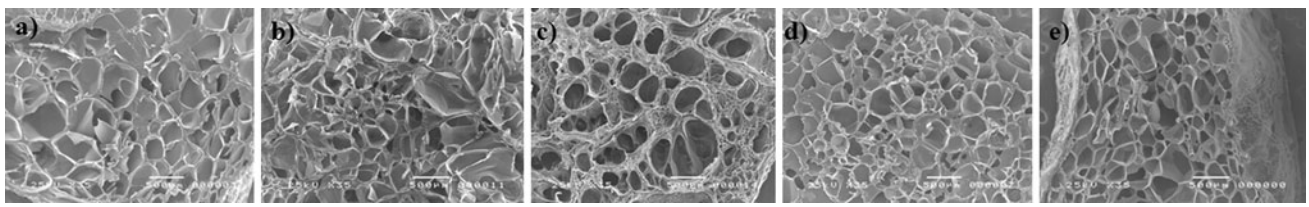

Fig. 3 SEM micrographs of CG hydrogels with increasing 5% GA content (v/v). **a** CG-3 (3%), **b** CG-3.5 (3.5%), **c** CG-4 (4%), **d** CG-4.5 (4.5%) and **e** CG-5 (5%)

that it degraded every 5 days ($P \leq 0.05$). However, the degree of degradation varied among samples with those that have higher GA content degraded slower. During the end of observation time, CG-3 lost about 90% of its original weight. The rest of samples degraded to less than 80% of its original weight (Fig. 6b).

3.3 Biocompatibility of the samples

3.3.1 Cytotoxicity

Cytotoxicity was determined using diluted extract solutions of the samples in accordance to ISO-10993-5 standards. It

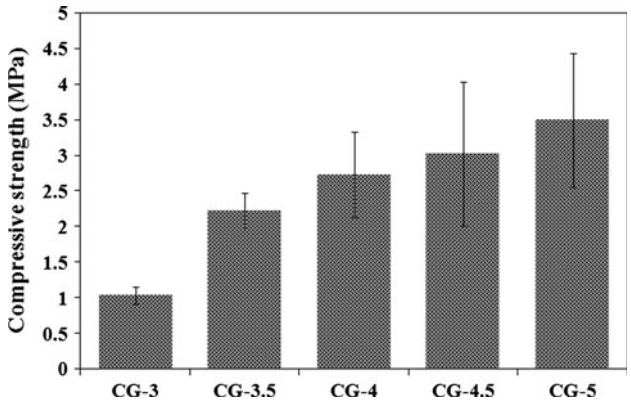

Fig. 4 Compressive strength of chitosan–gelatin hydrogels at different amount of GA crosslinker

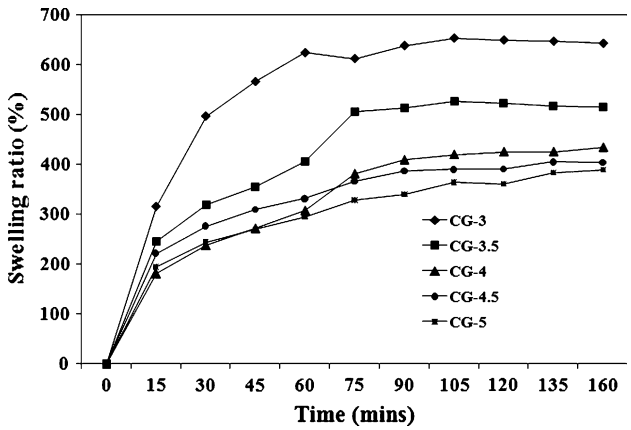

Fig. 5 Swelling kinetics of chitosan/gelatin hydrogels at different time intervals

can be observed that the PCL/PLGA membranes can support around 80% cell viability with 100% extract solution (Fig. 7a). In the case of CG hydrogels, gels with 4% and above GA content elicited cytotoxicity as evidenced by the drastic lowering of the cell viability when 100% extract solution was used ($P \leq 0.05$) (Fig. 7b).

3.3.2 Cell proliferation

The fibroblast cells used in this experiment were non-fastidious and did not display a lag phase during culture. Therefore, these cells were initially used to determine the ability of the materials to support cell viability and proliferation. Figure 8 showed that the PCL/PLGA membranes and CG hydrogel samples were able to support cell proliferation as indicated by the increased cell viability after 1, 3 and 5 days of culture. In the case of the membranes, cell growth was statistically significant every sampling day for all samples with the similar increase of cell growth except during the 5th day of culture when cell viability in M-12 exceeded the control ($P \leq 0.05$). Cells were observed to grow in number every sampling day ($P \leq 0.05$); however, there was an observed reduction in the fibroblast viability as a function of GA content in the CG hydrogels.

3.3.3 Cell adhesion behavior

Keratinocyte cells were used to demonstrate the ability of the PCL/PLGA membranes to support epidermal cell attachment and adhesion. Keratinocyte cells were shown to have a flattened morphology after 24 h of incubation, indicating that the cells recognized the cell adhesion sites in the membranes (Fig. 9). Continued cell adhesion was observed after 72 h with the deposition of extracellular material on the membrane fibers.

Figure 10 shows fibroblast cell growth on CG hydrogels. It was observed that the degree of growth was not the same for all hydrogels. In samples CG-3 and CG-3.5, cells were able to change shape drastically showing an outward

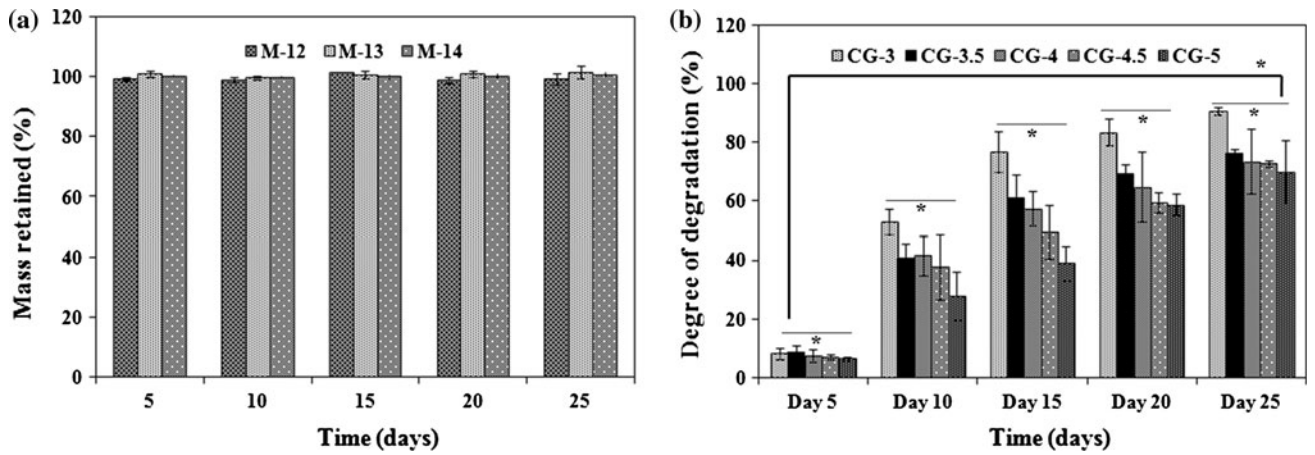

Fig. 6 In vitro biodegradation of **a** electro-spun PCL/PLGA membranes and **b** chitosan/gelatin hydrogels showing statistically significant weight changes of different samples at every sampling time ($^*P < 0.05$, $n = 4$)

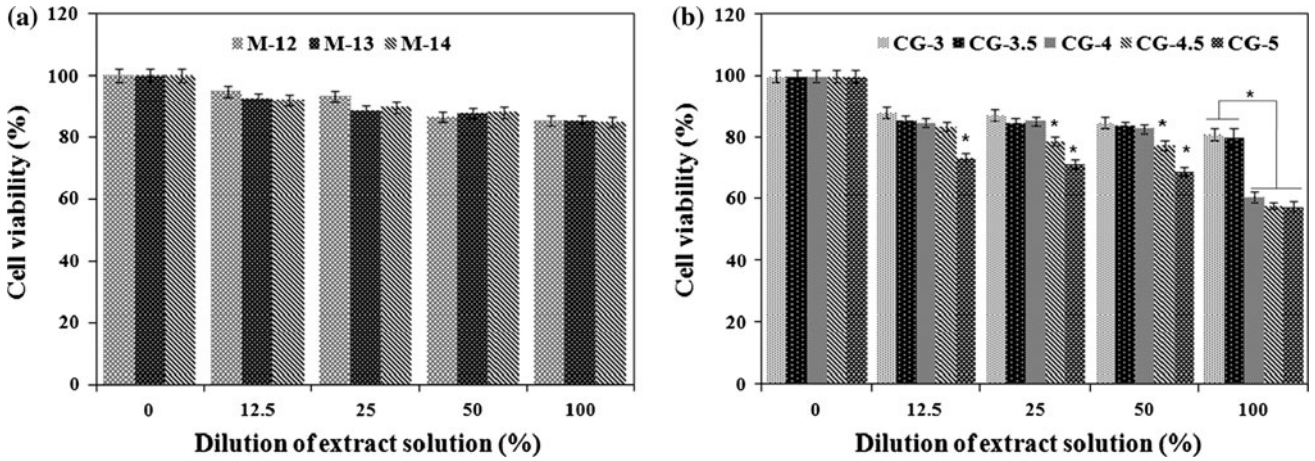

Fig. 7 Cytotoxicity of **a** PCL/PLGA membranes and **b** CG hydrogels at different concentrations of extract solutions. Cell viability from CG-4.5 and CG-5 extract solutions showed significantly reduced values ($*P < 0.05$, $n = 4$)

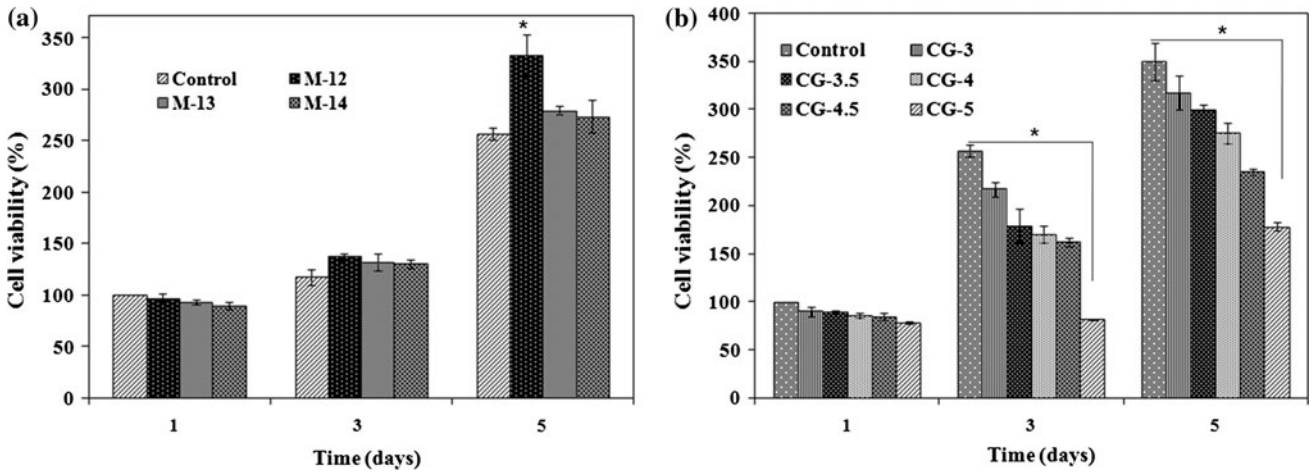

Fig. 8 Proliferation studies of fibroblast cells on **a** PCL/PLGA membranes with M-12 cell growth during 5th day of incubation and **b** chitosan/gelatin hydrogel showing decreasing cell growth with increasing crosslinker concentration ($*P < 0.05$, $n = 4$)

and bidirectional extension of extracellular material. In contrast, cell spreading on samples CG-4, CG-4.5 and CG-5 was limited even after 3 days.

3.4 Bilayer scaffold

In addition to examining the two biomaterials that will comprise the BS, preliminary data was also obtained on the constructed BS to determine if the bilayer composition affected the final structure of the material. Figure 11a, b shows the gross structure of BS prepared by underlaying of the membrane and casting of the hydrogel on the tissue culture plate. In these experiments, the membrane adhered to the hydrogel under dry conditions and followed the contour of the hydrogel surface.

The swelling behavior of BS followed that of the CG-3.5 (Fig. 11c). However, by measuring the size before and after swelling at 24 h, it was demonstrated that scaffold enlargement was minimized in the BS (table inserted) compared to the CGH alone. The biodegradation rate of BS was observed to be slower than that of the CG hydrogel (Fig. 11d). After 20 days, the degree of degradation of CG-3.5 was around 70% compared to around 60% for BS.

Figure 11d shows the cytotoxicity of BS compared to M-12 and CG-3.5. The cell viability was still to be around 80% with 100% extract solution. However, cell viability on BS was slightly reduced compared to its precursor materials.

4 Discussion

In this study, two different biomaterials were fabricated and characterized with the goal of fabricating a BS for skin tissue engineering applications. Based on an initial study from our laboratory [21] wherein the ratio of PCL and

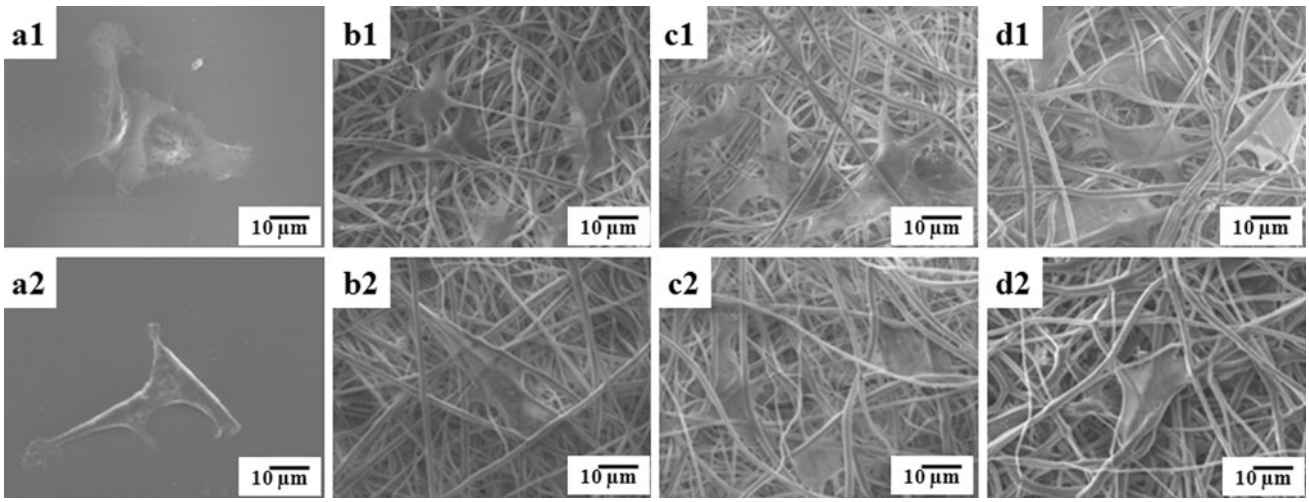

Fig. 9 Cell adhesion behavior of human keratinocyte cell (K155) on control TCP (**a**), M-12 (**b**), M-13 (**c**), M-14 (**d**) after 1 day (**a1–d1**) and 3 days of culture (**a2–d2**)

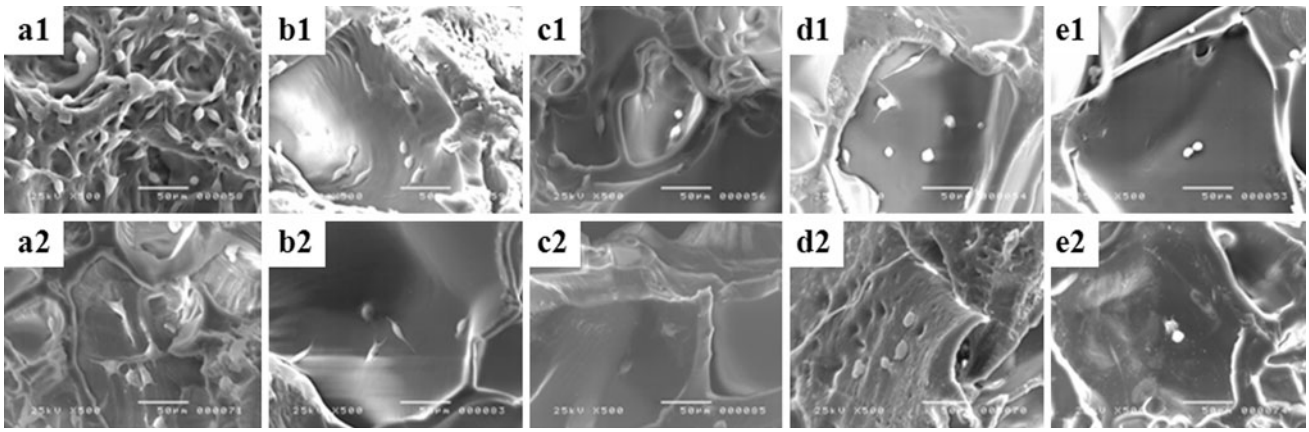

Fig. 10 Cell adhesion behavior of fibroblast cells CG-3 (**a**), CG-3.5 (**b**), CG-4 (**c**), CG-4.5 (**d**), CG-5 (**e**) after 1 day (**a1–e1**) and 3 days of culture (**a2–e2**)

PLGA was varied, the composition of the combined polymers was fixed at 80:20 but the effect of increasing the PCL concentration was investigated with the aim of optimizing its properties for tissue engineering scaffold applications. By increasing the PCL concentration, the mean fiber diameter and, consequently, the thickness and density of the fabricated membranes increased. The increased polymer concentration resulted in a higher viscosity of the electrospinning solution that may have produced more submicron-sized fibers that have meshed to form larger diameter fibers [22]. Compared to the pure electrospun PCL mats which displayed tensile strength of 1.40–2.10 MPa [23], the mechanical strength of the membranes fabricated in this study was improved when combined with PLGA (Table 1). It was noted, however, that the tensile strength of the material was reduced when the PCL concentration and, consequently, the fiber diameter was increased. As previously reported [24], an increase in fiber diameter resulted in a more dense material, which tends to break more easily during application of stress, as was the case in this study. Comparing it on previously published data of a preceding study [21], the discrepancy in the tensile strength of the M-12 maybe attributed to the difference in the preparation of the material particularly in the solvent combination used. The addition of methylene chloride in the membrane preparation produced tensile strength higher than Lee et al. with PCL [23] but lower than our laboratory publication prepared without methylene chloride.

Low viscosity chitosan at a concentration of 2% was used for ease of handling and for favorable mechanical strength as reported earlier [18]. Previous studies on chitosan–gelatin scaffolds have used gelatin concentrations of 1–5% [17, 25, 26]. However, we used 15% in this study based on the assumption that increased gelatin content may produce more favorable cell recognitions sites. Hydrogels were stabilized by the addition of glutaraldehyde as

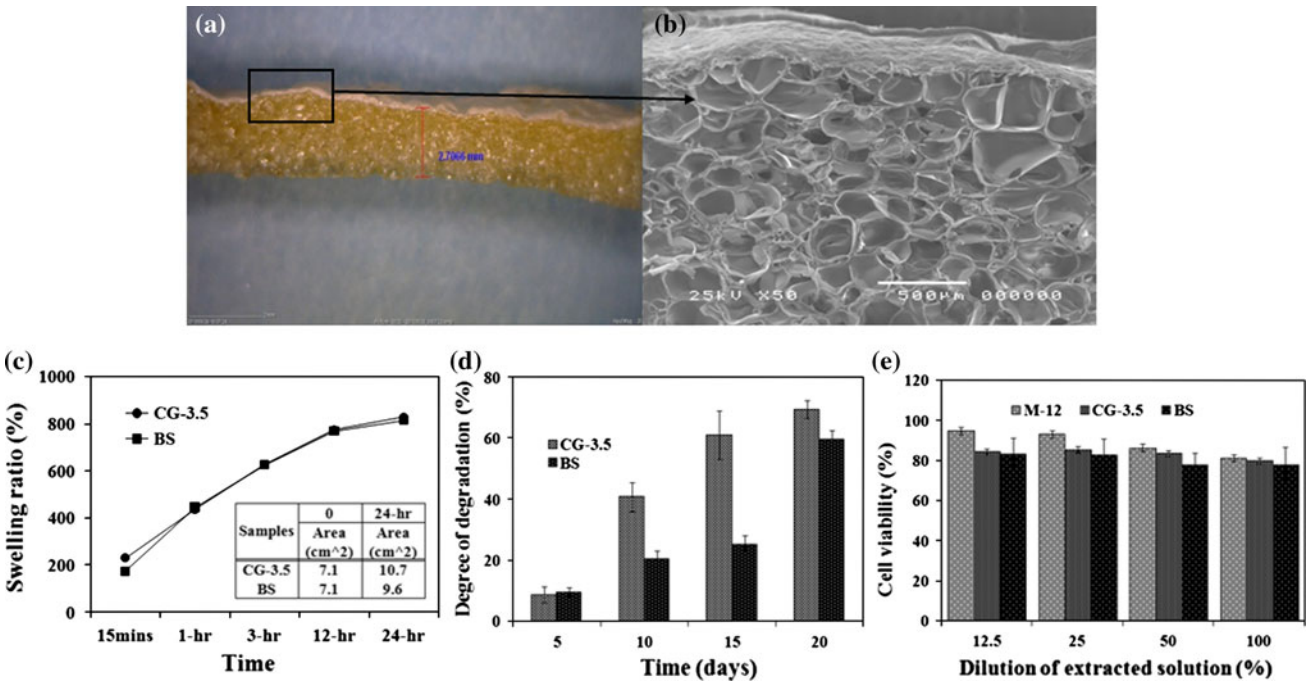

Fig. 11 Proposed BS structure (**a**, **b**) composed of an electrospun PCL/PLGA membrane and chitosan–gelatin hydrogel. Swelling and contraction (**c**), biodegradation (**d**) and cytotoxicity of BS using MTT assay (**e**)

crosslinking agent. The aldehyde groups of GA react with free amino groups of gelatin and chitosan forming a covalent bond which was shown to affect the mechanical integrity, physical properties as well as the biological interactions of the hydrogel but showed insignificant influence on the general morphology.

According to Shen et al., an original chitosan acetate and gelatin solution concentration of 2–5% can ensure porosity of 95–98% and that varying gelatin content was reported not to affect the porosity of the scaffold [27]. These conclusions were also observed in the hydrogel samples fabricated in this study, in which the porosity of the samples was close to 97%. The high gelatin concentration of 15% used in this study did not change the porosity relative to previously published values at lower gelatin concentrations. The varied amount of crosslinker added did not change the porosity and density values in all samples. Moreover, the average pore size diameter was also unaffected as the pore size is influenced by varying the by the pre-freezing temperature [15].

Hydrogels are normally crosslinked by chemical agents such as genipin [28–30], epoxy compounds [31], carbodiimide [30, 32, 33] and glutaraldehyde [34–36] to increase its mechanical stability. Glutaraldehyde serves as an effective crosslinking agent and was, therefore, chosen for this study. However, it is worth mentioning that glutaraldehyde can be cytotoxic at high concentrations so care should be given to how much is used during crosslinking [37]. GA was diluted to a 5% solution with deionized water and varying amounts was added to chitosan–gelatin hydrogels to investigate the appropriate concentration that will not induce cytotoxic effects but can maintain the structural integrity of the hydrogels.

The compressive strength of the hydrogels was observed to increase with the function of GA content which was due to the increased covalent crosslinks formed within the hydrogels that generated higher stresses for breakage. Deiber et al. reported that as the GA concentration was increased, the average mesh size is reduced so that the initial crack to break the hydrogel required higher tensions to materialize [38].

The ability of the hydrogels to absorb fluid to some extent is important for artificial skin functions, since this aid in the transfer of cell nutrients and metabolic products along the material during cell culture. Moreover, a moist wound environment also hasten wound healing rate because the tissues are prevented from being dessicated [39]. It was shown that a lower GA concentration allowed the hydrogel to swell more. This was also observed in a study conducted by Bigi et al. [34] with gelatin. Initially, water molecules hydrate the polar and hydrophilic groups of the hydrogel. As the maximal number of bound water is reached, the hydrogel network will try to accommodate more water which in this case was opposed by the

crosslinker. Consequently, as more water molecules occupy the hydrogel network there is a greater tendency for the network to break and disintegrate. Thus, if there is a greater opposing force, in this case, of the crosslinker present, a longer time is needed to completely disintegrate the hydrogel network.

The optimal degradation time rate of the scaffolds for use in the in artificial skin depends on its purpose and application. The proliferation phase of the wound healing process is said to be about 3 weeks [3]. Therefore, a scaffold intended for temporary skin replacement should not completely disintegrate before this time to be able to perform its template function. PCL is known to disintegrate for a long time, averaging 2 years, but the degradation rate decreases when PCL is combined with a co-polymer [11]. CG hydrogels, however, degrades relatively faster which can be expected from natural polymers.

The ability of the samples to support cell growth without inducing cytotoxic effects was evaluated using the MTT assay. For the PCL/PLGA membranes, no significant difference in the cytotoxicity was observed at increasing PCL concentrations. After 5 days of culture, it was observed that the membrane with the least amount of PCL was able to support the highest cell viability. This may be related to the amount of PCL used to fabricate the membrane. Increased PCL concentration produced fibers with larger diameter and fiber diameter was known to have an effect on cell growth, since fibers with larger diameters displayed reduced cell adhesion and limited cell proliferation [25]. In the case of CG hydrogels, the GA content significantly affected cell viability. Despite the high gelatin content, which was used to improve the cell affinity to the scaffold, a reduced cell viability was observed when the GA content was 4.5% and above. Optical inspection of the fibroblast cell morphology on the hydrogel samples can be correlated with the results of the MTT assay. Cell growth, as indicated by the change in cell shape and attachment of the extracellular material on the hydrogels, at lower GA content was significantly different compared to hydrogels at higher GA concentrations where cell shape did not drastically changed and attachment of the extracellular material was very limited. The mode of cytotoxic action of GA is dependent on its aldehyde groups. Loss of this reactive group will consequently reduce its biocidal activity [40]. A previous study reported that GA works by inducing DNA damage to some mammalian cell cultures [41].

A BS composed of two different materials can provide alternative methods for fabricating skin tissue engineering scaffolds. Commercially-available Integra is one example of a BS composed of a silicone upper layer and collagen-glycosaminoglycan sublayer. The structural principle shared by the BS being proposed in this study states that the upper layer imparts mechanical strength to the scaffold and acts as a wound cover while the lower layer helps to rehabilitate the wound environment. In contrast, the upper layer used in this study was composed of an electrospun PCL/PLGA membrane which is biodegradable and porous. These characteristics, especially biodegradability, can be controlled and modified for other purposes such as incorporation of a drug-delivery system which can help promote wound healing.

The CG hydrogel will comprise the bottom, porous layer. The CG hydrogel, due to its porous nature, can retain moisture which is beneficial in wound healing. In the preliminary data presented, enlargement and biodegradation were minimized in the BS compared with the CG hydrogel layer alone. This can be attributed with the adherence of the hydrophobic PCL/PLGA membrane layer that can resist water molecules in the upper surface of the BS structure rendering it to be relatively more stable in terms of shape changes and disintegration. The cell viability on the BS was around 80% but was observed to be slightly reduced compared to the PCL/PLGA membrane and CG hydrogel. This may be due to the combined effects of GA crosslinking and PCL hydrophobicity. Due to a relatively fast degradation rate of the CG hydrogel layer, the BS cannot withstand long term cell culture when used as a cellularised tissue engineering scaffold. As an acellular scaffold aimed to aid wound healing, the fabricated BS has shown favorable in vitro biocompatibility. However, the effects of degradation by-products and material behavior in vivo must still be investigated.

5 Conclusion

Two separate biomaterials were fabricated and characterized to investigate on the qualities that can support a BS for future skin tissue engineering applications. A bilayer design was envisioned for an artificial skin scaffold where distinct qualities of the two systems can be combined to enhance its function. The electrospun PCL/PLGA membrane (M-12) displayed the best mechanical strength and biocompatible properties. The chitosan–gelatin hydrogel (CG-3.5) is a porous and absorbable scaffold that can support relatively high cell viability while maintaining important physical properties (mechanical strength and degradation) required for a skin tissue scaffold. The proposed combination of these two biomaterials can open more possibilities for wound treatment and rehabilitation as one system may not be sufficient to answer the complex environment in wound treatment and skin regeneration.

Acknowledgment This work was supported by Mid-career Research Program through NRF grant funded by MEST (NO 2009-0092808).

References

1. Tabata Y. Recent progress in tissue engineering. Drug Discov Today. 2001;6:483–7.
2. Böttcher-Haberzeth S, Biedermann T, Reichmann E. Tissue engineering of skin. Burns. 2009;36:450–60.
3. Veen Vvd, van der Wal MB, van Leeuwen MC, Ulrich MM, Middelkoop E. Biological background of dermal substitutes. Burns. 2009;36:305–21.
4. Nangia A, Gambhir R, Maibach H. Factors affecting the performance of temporary skin substitutes. Clin Mater. 1991;7:3–13.
5. Agarwal S, Wendorff J, Greiner A. Use of electrospinning technique for biomedical applications. Polymer. 2008;49:5603–21.
6. Venugopal J, Ramakrishna S. Applications of polymer nanofibers in biomedicine and biotechnology. Appl Biochem Biotechnol. 2005;125:147–58.
7. Liang D, Hsiao B, Chu B. Functional electrospun nanofibrous scaffolds for biomedical applications. Adv Drug Deliv Rev. 2007;59:1392–412.
8. Eshragi S, Das S. Mechanical and microstructural properties of polycaprolactone scaffolds with one-dimensional, two-dimensional, and three-dimensional orthogonally oriented porous architectures produced by selective laser sintering. Acta Biomater. 2010;6:2467–76.
9. Sahoo S, Sasmal A, Nanda R, Phani AR, Nayak PL. Synthesis of chitosan-polycaprolactone blend for control delivery of ofloxacin drug. Carbohydr Polym. 2010;79:106–13.
10. Khor HL, Ng KW, Schantz JT, Phan TT, Lim TC, Teoh SH, Hutmacher DW. Poly(ε-caprolactone) films as a potential substrate for tissue engineering an epidermal equivalent. Mater Sci Eng C. 2002;20:71–5.
11. Woodruff MA, Hutmacher D. The return of a forgotten polymer—polycaprolactone in the 21st century. Prog Polym Sci. 2010;35:1217–56.
12. Kumbar S, Nukavarapu S, James R, Nair L, Laurencin C. Electrospun poly(lactic acid-co-glycolic acid) scaffolds for skin tissue engineering. Biomaterials. 2008;29:4100–7.
13. Mi F, Lin Y, Wu Y, Shyu S, Tsai Y. Chitin/PLGA blend microspheres as a biodegradable drug-delivery system: phase-separation, degradation and release behavior. Biomaterials. 2002;23:3257–67.
14. Mao J, Zhao L, De Yao K, Shang Q, Yang G, Cao Y. Study of novel chitosan–gelatin artificial skin in vitro. J Biomed Mater Res. 2003;64A:301–8.
15. Mao JS, Zhao L, Yin YJ, Yao KD. Structure and properties of bilayer chitosan–gelatin scaffolds. Biomaterials. 2003;24:1067–74.
16. Chen T, Embree H, Brown EM, Taylor MM, Payne GF. Enzyme-catalyzed gel formation of gelatin and chitosan: potential for in situ applications. Biomaterials. 2003;24:2831–41.
17. Chang Y, Xiao L, Tang Q. Preparation and characterization of a novel thermosensitive hydrogel based on chitosan and gelatin blends. J Appl Polym Sci. 2009;113:400–7.
18. Kathuria N, Tripathi A, Kar K, Kumar Ashok. Synthesis and characterization of elastic and macroporous chitosan–gelatin cryogels for tissue engineering. Acta Biomater. 2009;5:406–18.
19. Muzzarelli R. Chitins and chitosan for the repair of wounded skin, nerve, cartilage and bone. Carbohydr Polym. 2009;76:167–82.
20. Lee S. Bio-artificial skin composed of gelatin and (1→3), (1→6)-β-glucan. Biomaterials. 2003;24:2503–11.
21. Hiep N, Lee B-T. Electro-spinning of PLGA/PCL blends for tissue engineering and their biocompatibility. J Mater Sci Mater Med. 2010;21(6):1969–78.
22. Saraf A, Lozier G, Haesslein A, Kasper FK, Raphael RM, Baggett LS, Mikos AG. Fabrication of nonwoven coaxial fiber meshes by electrospinning. Tissue Eng Part C. 2009;15(3):333–44.
23. Lee KH, et al. Characterization of nano-structured poly([var epsilon]-caprolactone) nonwoven mats via electrospinning. Polymer. 2003;44(4):1287–94.
24. Kwon IK, Kidoaki S, Matsuda T. Electrospun nano- to microfiber fabrics made of biodegradable copolyesters: structural characteristics, mechanical properties and cell adhesion potential. Biomaterials. 2005;26:3929–39.
25. Ma J, Wang H, He B, Chen J. A preliminary in vitro study on the fabrication and tissue engineering applications of a novel chitosan bilayer material as scaffold of human neofetal dermal fibroblasts. Biomaterials. 2001;22:331–6.
26. Huang Y, Onyeri S, Siewe M, Moshfeghian A, Madihally S. In vitro characterization of chitosan–gelatin scaffolds for tissue engineering. Biomaterials. 2005;26:7616–27.
27. Shen F, Cui Y, Yang LF, Yao KD, Dong XH, Jia WY, Shi HD. A study on the fabrication of porous chitosan/gelatin network scaffold for tissue engineering. Polym Int. 2000;49:1596–9.
28. Bigi A, Cojazzi G, Panzavolta S, Roveri N, Rubini K. Stabilization of gelatin films by crosslinking with genipin. Biomaterials. 2002;23:4827–32.
29. Song F, Zhang L, Yang C, Yan L. Genipin-crosslinked casein hydrogels for controlled drug delivery. Int J Pharm. 2009;373:41–7.
30. Liang H, Chang W, Liang H, Lee M, Sung H. Crosslinking structures of gelatin hydrogels crosslinked with genipin or a water-soluble carbodiimide. J Appl Polym Sci. 2004;91:4017–26.
31. Sung HW, Hsu C, Lee YS, Lin DS. Crosslinking characteristics of an epoxy-fixed porcine tendon: effects of pH, temperature, and fixative concentration. J Biomed Mater Res. 1996;31:511–8.
32. Xu JB, Bartley J, Johnson RA. Preparation and characterization of alginate-carageenan hydrogel films crosslinked using a water soluble carbodiimide (WSC). J Membr Sci. 2003;218:131–46.
33. Hu X, Zhou J, Zhang N, Tan H, Gao C. Preparation and properties of an injectable scaffold of poly(lactic-co-glycolic acid) microparticles/chitosan hydrogel. J Mech Behav Biomed Mater. 2008;1:352–9.
34. Bigi A, Cojazzi G, Panzavolta S, Rubini K, Roveri N. Mechanical and thermal properties of gelatin films at different degrees of glutaraldehyde crosslinking. Biomaterials. 2001;22:763–8.
35. Azab AK, Orkin B, Doviner V, Nissan A, Klein M, Srebnik M, Rubinstein A. Crosslinked chitosan implants as potential degradable devices for brachytherapy: in vitro and in vivo analysis. J Control Release. 2006;111:281–9.
36. Rohindra D, Nand A, Khurma J. Swelling properties of chitosan hydrogels. S Pac J Nat Sci. 2004;22:32–5.
37. Jayakrishnan A, Jameela S. Glutaraldehyde as a fixative in bioprostheses and drug-delivery matrices. Biomaterials. 1996;17:471–84.
38. Deiber J, Ottone M, Piaggio M, Peirotti M. Characterization of cross-linked gelatin hydrogels through the rubber elasticity and thermodynamic swelling theories. Polymer. 2009;50:6065–75.
39. Noorjahan SE, Sastry TP. An in vivo study of hydrogels based on physiologically clotted fibrin–gelatin composites as wound-dressing materials. J Biomed Mater Res B. 2004;71B(2):305–12.
40. Gorman SP, Scott E, Russell AD. A review: antimicrobial activity, uses and mechanism of action of glutaraldehyde. J Appl Bacteriol. 1980;48:161–90.
41. Zeiger E, Gollapudi B, Spencer P. Genetic toxicity and carcinogenicity studies of glutaraldehyde—a review. Mutat Res. 2005;589:136–51.